First-principles study of the electronic structures and optical properties of C–F–Be doped wurtzite ZnO

Zuo Chunying(左春英)[1,†], Wen Jing(温静)[1], and Zhong Cheng(钟成)[2]

[1]College of Science, Heilongjiang Bayi Agricultural University, Daqing 163319, China
[2]College of Chemistry and Molecular Sciences, Wuhan University, Wuhan 430072, China

Abstract: The electronic structure and optical properties of pure, C-doped, C–F codoped and C–F–Be cluster-doped ZnO with a wurtzite structure were calculated by using the density functional theory with the plane-wave ultrasoft pseudopotentials method. The results indicate that p-type ZnO can be obtained by C incorporation, and the energy level of C_O above the valence band maximum is 0.36 eV. The ionization energy of the complex $Zn_{16}O_{14}CF$ and $Zn_{15}BeO_{14}CF$ can be reduced to 0.23 and 0.21 eV, individually. These results suggest that the defect complex of $Zn_{15}BeO_{14}CF$ is a better candidate for p-type ZnO. To make the optical properties clear, we investigated the imaginary part of the complex dielectric function of undoped and C–F–Be doped ZnO. We found that there is strong absorption in the energy region lower than 2.7 eV for the C–F–Be doped system compared to pure ZnO.

Key words: first-principles; electronic structures; optical properties; wurtzite ZnO
DOI: 10.1088/1674-4926/33/7/072001 **PACC:** 7115A; 7115M; 7115H

1. Introduction

Wurtzite-ZnO, a direct wide-gap (3.37 eV) semiconductor with an excition binding energy of 60 meV, is a promising material due to its superior electronic, optical, and piezoelectric properties, leading to novel applications in the fields of blue and UV lasers, light emitting diodes, solid state lighting, and transparent conducting contacts[1−6].

The fabrication of n-ZnO has proved to be easy because of the existence of Zn interstitials and O vacancies. However, it is difficult to obtain p-type ZnO because of its spontaneous defects compensation effect between the acceptor dopants and intrinsic donors[7], low solubility of the acceptor dopants[8] and relatively deep acceptor levels[9]. Recently, it has been shown that the problem of low dopant solubility can sometimes be resolved by non-equilibrium growth techniques, such as molecular doping or epitaxy[9−11]. In order to decrease the ionization energy of the acceptor, codoping and even the cluster-doping method have become hotspots of the research on p-type ZnO[2, 12−15].

The main aim of this paper is to find a suitable impurity, which can increase the solubility of the acceptor dopants and reduce the acceptor level of p-type ZnO. Because a C atom has four valence electrons with two electrons less than O atom, C provides two holes when substituting an O atom. We chose C as the double acceptor[16] in order to avoid the repulsion interaction between acceptors in the present paper. Fluorine, the radius of which is close to that of oxygen, could be an appropriate anion doping candidate[17]. In addition, considering that F has a lower p orbital energy than O[9], we used F to substitute for the O atom adjacent to C. Li *et al.*[9] found that the acceptor transition energy could be shallower when a Zn atom is replaced next to the acceptor by isovalent Be in order to reduce the anion and cation p–d coupling. Gai *et al.*[18] have also suggested that the acceptor of N transition energy could be reduced by substituting the surrounding Zn with isovalent Mg. It is well known that crystal lattice mismatching can increase impurity formation. In view of these points, we replaced one Zn atom by isovalent Be to reduce the p–d repulsion between the C acceptor and the Zn atom. For C–F–Be cluster doped ZnO, to our knowledge, there have been no experimental or theoretical investigations. In this paper, the lattice parameters, the band structure, the density of states (DOS), bond population, impurity formation energy, the acceptor transition energy, and optical property of undoped and doped wurtzite ZnO will be investigated.

2. Theoretical model and computational method

2.1. Theoretical model

Ideal ZnO has a hexagonal wurtzite structure at ambient temperature and pressure and it belongs to the $P6_3mc$ space group and C_{6v}^4 symmetry. The cell parameters are $a = b = 3.25$ Å, $c = 5.20$ Å, $c/a = 1.60$, $\alpha = \beta = 90°$, and $\gamma = 120°$[19].

The supercell ($2 \times 2 \times 2$) adopted contains 16 Zn and 16 O atoms in the calculation in order to construct C-doped, C–F codoped and C–F–Be cluster-doped structures. In this paper, we took four different configurations, as shown in Fig. 1.

2.2. Calculation methods

Our calculations are carried out by using the first-principles pseudopotential method based on the density function theory (DFT)[20], as implemented in the CASTEP code[21], which is widely used for a variety of crystal systems and has been successfully applied to ZnO[22−26]. The generalized gradient approximation (GGA) as proposed by

† Corresponding author. Email: chunyingzuo3010@126.com
Received 25 November 2011, revised manuscript received 13 February 2012

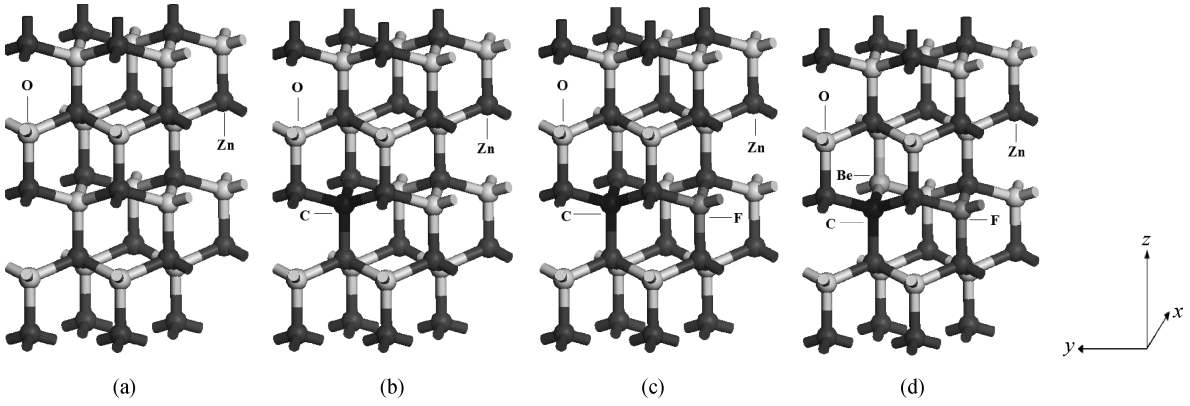

Fig. 1. Crystal structures of supercells for (a) pure ZnO, (b) ZnO:C, (c) ZnO:C–F and (d) ZnO:C–F–Be.

Table 1. Comparison of the optimized results of the primitive cell of undoped ZnO in the present paper with other theoretical values and experimental data (LDA refers to local density approximation and HSE means high-speed experimentation approach).

Parameter	a (Å)	c (Å)	c/a	Volume (Å^3)
Present paper (GGA functional)	3.303	5.287	1.601	49.829
Computed value (GGA functional)[29]	3.283	5.298	1.614	49.461
Computed value (sX-LDA functional)[29]	3.249	5.205	1.602	47.595
HSE approach[29]	3.230	5.250	1.625	—
Experimental value[19, 30, 31]	3.250	5.207	1.602	48.335

Table 2. Optimized lattice parameters and calculated formation energy for doped ZnO.

Parameter	$Zn_{16}O_{15}C$	$Zn_{16}O_{14}CF$	$Zn_{15}BeO_{14}CF$
a (Å)	3.303	3.319	3.298
c (Å)	5.307	5.324	5.285
c/a	1.607	1.604	1.602
Volume (Å^3)	50.032	50.625	49.608
Formation energy (eV)	2.37	1.70	2.73

Perdew, Burke, and Ernzerhof (PBE)[21, 27] was applied, combined with Vanderbilt ultrasoft pseudopentials[28]. A $5 \times 5 \times 4$ Monkhorst–Pack grid is used for Brillouin-zone sampling, together with an energy cutoff of plane wave of 360 eV, which are both within convergence.

3. Results and discussion

3.1. Geometric structure and formation energy

First, we optimized internal coordinates after optimization of the lattice parameters in pure ZnO to obtain stable and accurate results. The optimized results of the primitive cell of undoped ZnO are illustrated in Table 1.

It is observed that the optimized lattice parameters are in good agreement with the experimental and other theoretical values, which assures the reliability of our calculations.

It is necessary to calculate the formation energy and analyze lattice parameters which can be described accurately by using DFT calculations, because they reflect the stability of alloys. The formation energy of impurity α in a neutral state is defined as

$$\Delta H_{\rm f} = E(\alpha) - E(0) + \Delta n_{\rm zn}\mu_{\rm zn} + \Delta n_{\rm O}\mu_{\rm O} + \sum_i \Delta n_i \mu_i, \quad (1)$$

where $E(\alpha)$ and $E(0)$ are the total energies of the supercell with and without the impurity α and i = C, F or Be. Quantities Δn_X and μ_X are the number of species X (= Zn, O, C, F, Be) removed from a perfect cell to its respective reservoir to form the impurity cell and the corresponding reservoir chemical potential, respectively. Changes in these chemical potentials will affect the magnitude of the formation energy but not the value of the acceptor level. The chemical potentials $\mu_{\rm Zn}$, $\mu_{\rm O}$, $\mu_{\rm F}$, $\mu_{\rm Be}$ and $\mu_{\rm C}$ may not exceed the energies of hcp Zn, bulk Be, gaseous O_2, F_2, and graphite C. They are offset to zero in the present study. In equilibrium the restriction on the chemical potentials for ZnO is $\mu_{\rm O} + \mu_{\rm Zn} = \mu_{\rm ZnO}$. Our more accurate calculation gives $\mu_{\rm ZnO} = -3.59$ eV (with respect to hcp Zn and gaseous O_2), which is consistent with the experimental data[19, 30, 31] and the other theoretical value[17] . These conditions limit the range of $\mu_{\rm O}$ or $\mu_{\rm Zn}$ in $-3.59 < \mu_{\rm O,\,Zn} < 0$. Under the O-rich condition ($\mu_{\rm O} = 0$), $\mu_{\rm Be}^{\rm max}$ can be determined by $\mu_{\rm BeO}$. Our more accurate calculation gives $\mu_{\rm Be}^{\rm max} = -5.73$ eV (with respect to bulk Be and gaseous O_2). Based on these limits, the calculated formation energies for $Zn_{16}O_{15}C$, $Zn_{16}O_{14}CF$, and $Zn_{15}BeO_{14}CF$ are listed in Table 2.

For $Zn_{16}O_{15}C$, the lattice parameters and primitive cell volume increase compared with pure ZnO. This phenomenon occurs because the atomic radius of C (0.91 Å) is larger than that of O (0.65 Å). Comparing $Zn_{16}O_{15}C$ with $Zn_{16}O_{14}CF$,

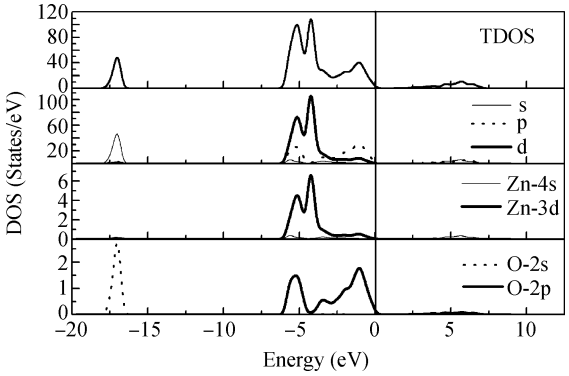

Fig. 2. Density of states of pure ZnO.

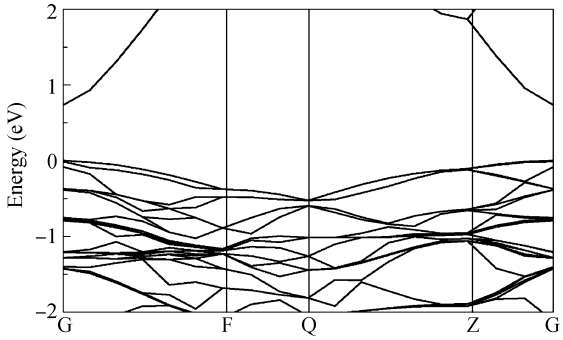

Fig. 3. Band structure of pure ZnO.

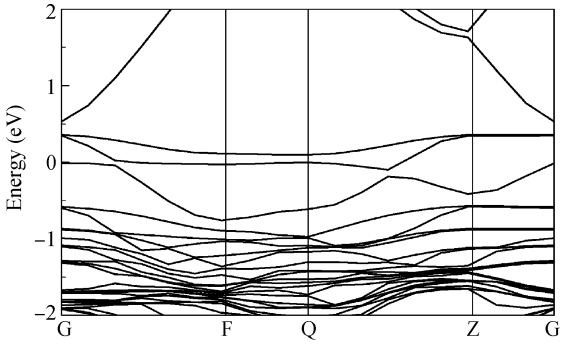

Fig. 4. Band structure of $Zn_{16}O_{15}C$.

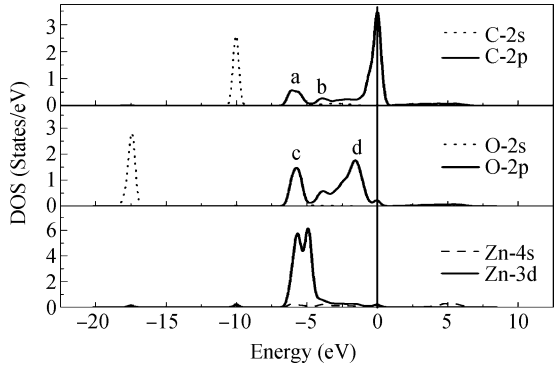

Fig. 5. Density of states of $Zn_{16}O_{15}C$.

the lattice parameters *a* and *c* increase 0.48% and 0.32%, respectively, as F incorporation due to the formation of a strong ionic bond between F and Zn. These results suggest that C–F codoped method induces the lattice mismatch of ZnO. When Be is incorporated into C–F codoped ZnO, the lattice parameters *a* and *c* become closer to the values of pure ZnO. The calculated errors for the lattice constants *a* and *c* are 0.15% and 0.038%, respectively, which shows that the phenomenon of lattice mismatch is improved at a large extent.

3.2. Electronic structure of pure ZnO

In this paper, the Fermi level indicated by a solid line is set as zero.

For undoped ZnO, it is observable from Fig. 2 that the valence band can be divided into two groups. The upper valence band (−3.80 to 0.01 eV) originates mainly from O2p states with a small contribution from Zn3d states; the lower valence band (−6.16 to −3.80 eV) with a strong d character is mainly formed by 3d states of Zn. The conduction band is mainly from the Zn4s states with fewer O2p states, which is consistent with the experimental results[32]. It should be noticed that there are double split peaks composed of 3d states of Zn in the energy range of −6.07 and −3.69 eV.

Figure 3 shows the band structure of pure ZnO. It is evident that the direct band gap is about 0.73 eV at the highly symmetric G(Γ) point, which is consistent with the earlier calculated results[33−36], and it is less than the experimental value of 3.37 eV. It is well known that the underestimated band gap can be due to neglect of the correlation between excited-state electrons. The LDA(GGA)+U method is known to be able to correct band-gap errors by applying a potential to the outer d electrons of transition metals[37]. Since we do not have accurate experimental measurements of the band gaps of the C–F–Be doped ZnO and because we are interested in the qualitative impact of dopants on the band gap, it was decided that the GGA+U method was not useful in the present paper[38]. The lower valence band from mainly Zn3d states changes slowly because the 3d states of Zn are full of electrons. Compared with the conduction band from Zn4s states, the gentle change of the upper valence band from the O2p states illustrates that the holes in valence band have a fairly large effective mass, which is one of the main reasons for the difficulty in the realization of p-type ZnO[39].

The narrow valence band region located at –17.02 eV from 2s states at O sites is not discussed because of its weak interaction with other electron states.

3.3. Electric structure of C-doped, C–F codoped and C–F–Be cluster-doped wurtzite ZnO

Firstly, we replaced one O atom in a ZnO supercell by C. The band structure and DOS of $Zn_{16}O_{15}C$ system are illustrated in Figs. 4 and 5.

For the $Zn_{16}O_{15}C$ system, Figure 4 clearly shows that the conduction band minimum and valence band maximum are at the same *k*-point and the value of band gap obtained in the work is 0.55 eV. It confirms that when a C atom is substitutionally doped at the O site in the bulk ZnO, the band gap becomes narrow, which is consistent with the value of Ref. [31].

Compared with the DOS of undoped ZnO in Fig. 3, a new narrow band exists near −9.96 eV, which is mainly from C2s

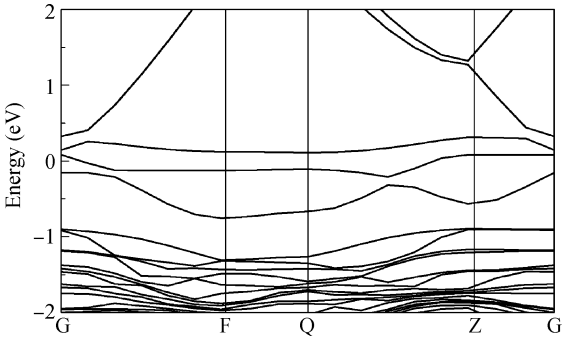

Fig. 6. Band structure of $Zn_{16}O_{14}CF$.

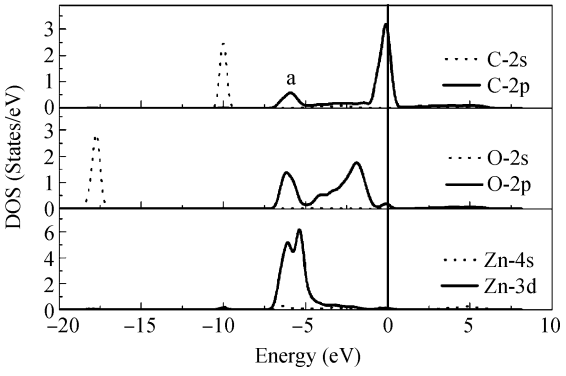

Fig. 7. Density of states of C, O and Zn of C–F codoped ZnO.

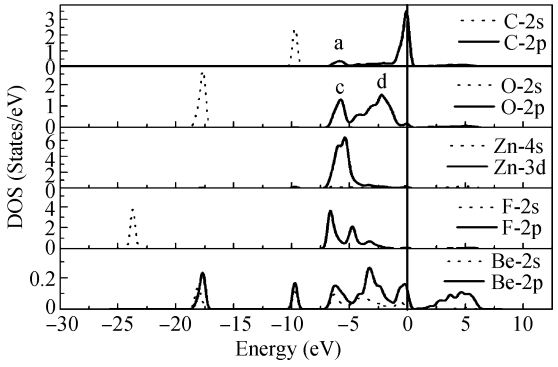

Fig. 8. Density of states of $Zn_{15}BeO_{14}CF$.

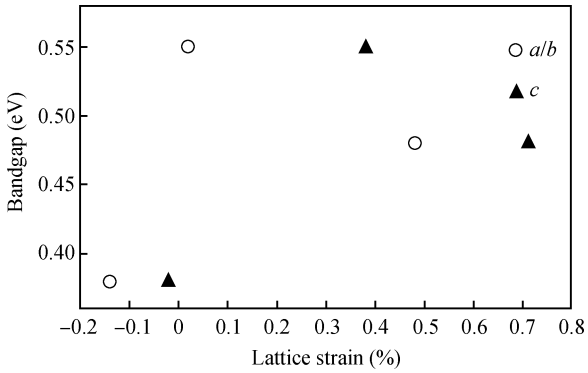

Fig. 9. Bandgap energy as a function of strain in *a*/*b* and *c* axis directions.

states with a little Zn4s and Zn3d effect. This shows that C2s, Zn4s and Zn3d states have a strong coupling effect. It is clear that there is a strong orbital overlap in the energy region of −6.83 to 0.41 eV for Zn3d, C2p and O2p states. For Zn3d and O2p states in pure ZnO, the orbital overlap region is from −6.37 to −0.01 eV. It can be noticed from these results that C easily binds with Zn and O, which is also verified by the bond population number. It is obvious that another peak appears in the energy region of −0.44 to 0.54 eV for O2p states and the cleavage strength of Zn3d states becomes weaker when C is incorporated into ZnO. Moreover, the most important point to be noted is that the DOS near the Fermi level increases, which originates mainly from the C2p states. This result indicates that p-type ZnO can be achieved by C-doping. The level of C_O in ZnO is at about 0.36 eV above the valence band maximum (VBM). Although C_O supplies holes at the top of the valence band, it forms a relatively deep acceptor level above VBM. Therefore, it cannot be easily ionized, which shows that it cannot contribute to obtaining high quality p-type ZnO.

In order to reduce the energy level of C_O, we replaced one of the nearest neighboring O atoms by the more electronegative F in $Zn_{16}O_{15}C$ system. F incorporation induces a shallower level of C_O (0.23 eV above the VBM) according to the band structure calculation, as seen in Fig. 6.

Figure 7 shows the DOS in the C–F codoped ZnO configuration. When incorporating F into ZnO, for C2p states, it is worth noting that the "*a*" peak in Fig. 5 in the energy range from −6.83 to −4.74 eV becomes wider and the "*b*" peak in Fig. 5 in the energy range from −4.74 to −3.17 eV has disappeared. The cleavage strength of O2p states in the energy range from −4.67 to −0.38 eV becomes weaker.

Taking account of p–d coupling interaction in C2p and Zn3d orbitals, we replaced one of the nearest neighboring Zn atom by isovalent Be in $Zn_{16}O_{14}CF$ system.

Comparing to the case of $Zn_{16}O_{14}CF$, the transition energy of C_O reduces to 0.21 eV when incorporating Be into the system. The acceptor transition energy is shallower when a Zn atom is replaced next to the acceptor by isovalent Be because the anion and cation p–d coupling is reduced. These results suggest that the defect complex of $Zn_{15}BeO_{14}CF$ is a better candidate for p-type ZnO.

Figure 8 gives the DOS in the $Zn_{15}BeO_{14}CF$ configuration.

It is clearly observed that the splitting peak of the DOS for Zn3d has almost disappeared. We know that the Be has no occupied d orbital, therefore, the hybridization between the Zn3d, C2p, and O2p states is decreased with Be doping. Comparing to the partial DOS of C in $Zn_{16}O_{15}C$ in Fig. 5, the "*a*" peak has shifted to a higher energy range slightly and the "*b*" peak has almost disappeared. Furthermore, comparing with Fig. 5, the "*c*" peak has moved to a higher energy region, but the "*d*" has moved to the opposite direction. It can be noticed from these results that there is strong orbital coupling between the 2s and 2p states of C, O2p and Be2p states.

In this paper, we also investigate the effect of strain on the bandgap. Figure 9 depicts the relation between bandgap and lattice strain for doped systems. It is observed that tensile strain and compressive strain in the direction of *a* and *c* axises both induce a narrower bandgap compared with undoped ZnO. Therefore, the statement that compressive strain

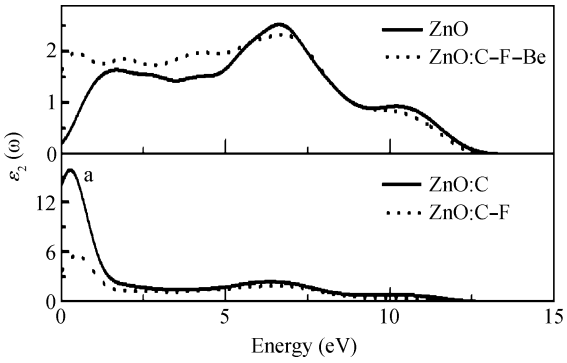

Fig. 10. Imaginary part of dielectric function $\varepsilon_2(\omega)$ of pure and C–F–Be doped ZnO.

makes the bandgap widen and tensile strain leads to a smaller bandgap[40] needs further investigation.

3.4. Optical properties of undoped and C–F–Be doped ZnO

It is well known that the interaction of a photon with the electrons in a system can be described in the light of time-dependent perturbations of the ground-state electronic states. The imaginary part $\varepsilon_2(\omega)$ of the dielectric function can be calculated from momentum matrix elements between the occupied and unoccupied states. The real part $\varepsilon_1(\omega)$ of the dielectric function can be achieved from the imaginary part $\varepsilon_2(\omega)$ according to the famous Kramer–Kronig relationship. All the other optical constants can be derived from $\varepsilon_1(\omega)$ and $\varepsilon_2(\omega)$. Therefore, work was devoted entirely to the characters of the imaginary part $\varepsilon_2(\omega)$ of the dielectric function for undoped and C–F–Be doped ZnO. In our calculation, we have used the scissor approximation to fit the calculated absorption edge to the experimental value.

The calculated imaginary parts $\varepsilon_2(\omega)$ of the dielectric function of pure and C–F–Be doped ZnO are exhibited in Fig. 10. It can be used to describe the real transitions between occupied and unoccupied electronic states.

It is found from the calculated $\varepsilon_2(\omega)$ spectra that there are three main absorption peaks for pure ZnO. The first absorption peak, located at about 3.3 eV, mainly comes from the electron transition between the O2p and Zn4s orbitals. The second absorption peak at about 8.4 eV can be due to the transition between the Zn3d and O2p orbitals. The highest peak at about 11.5 eV is mainly derived from the optical transition between the Zn-3d and the highest orbitals. Our calculated results are in good agreement with the experimental data[41] and they are also consistent with other theoretical values[42].

After incorporating C–F–Be into the system, there is a higher peak at about 2.1 eV, which shows that C–F–Be doped ZnO system should have interesting characteristics in this low-energy region. By comparison with undoped ZnO, the first peak for pure ZnO shifts to the lower energy region (red shift), which is in good agreement with the result of the DOS. Compared with pure ZnO, the optical transition has been enhanced for C–F–Be doped ZnO. All of these results show that the $Zn_{15}BeO_{14}CF$ configuration has potential application in optical materials.

4. Conclusion

In this paper, the supercells of undoped and doped ZnO were calculated by using the Perdew-burke-Ernzerhof form of the generalized gradient approximation within the framework of density functional theory. The effects of C doping, C–F codoping and C–F–Be cluster-doping on the crystal structure, formation energy, electronic structure, optical properties, and the relation between strain and bandgap were evaluated on the basis of calculated data.

By comparing with the lattice parameters of pure ZnO, C and C–F incorporations lead to a volume increase. However, the lattice volume is basically in accordance with that of pure ZnO after incorporating Be into the $Zn_{16}O_{14}CF$ system. The calculated results show that p-type ZnO can be obtained by C incorporation. The energy level of C_O above the valence band maximum and the formation energy are 0.36 and 2.37 eV, respectively, for C-doped ZnO. When incorporating the more electronegative F as the reactive donor into the $Zn_{16}O_{15}C$ system, the formation and ionization energies can be reduced to 1.70 and 0.23 eV, individually. Compared with the system of C–F codoped ZnO, when replacing one Zn atom with the isovalent Be without d-orbit, the formation and ionization energies of the complex $Zn_{15}BeO_{14}CF$ are 2.73 and 0.21 eV, respectively. By investigating the imaginary part of the dielectric function, we found that there is strong absorption in the energy region lower than 2.7 eV for C–F–Be doped systems by comparison with pure ZnO.

This work will have important significance for better understanding and further developing ZnO, which has better p-type conductive characteristics and displays interesting behavior in the low energy region when C–F–Be is incorporated into it.

References

[1] Zhang X D, Guo M L, Liu C L, et al. First-principles investigation of electronic and optical properties in wurtzite $Zn_{1-x}Mg_xO$. Phys J B, 2008, 62: 417

[2] Wang L G, Zunger A. Cluster-doping approach for wide-gap semiconductors: the case of p-type ZnO. Phys Rev Lett, 2003, 90: 256401

[3] Gupta A, Verma N K, Bhatti H S. Fast photoluminescence decay processes of doped ZnO phosphors. J Low Temp Phys, 2007, 14: 749

[4] Yoshino K, Hata T, Kakeno T, et al. Electrical and optical characterization of n-type ZnO thin films. Phys Status Solidi C, 2003, 0(2): 626

[5] Nomura K, Ohta H, Ueda K, et al. Thin-film transistor fabricated in single-crystalline transparent oxide semiconductor. Science, 2003, 300: 1269

[6] Huang M H, Mao S, Feick H, et al. Room-temperature ultraviolet nanowire nanolasers. Science, 2001, 292: 1897

[7] Zhang S B, Wei S H, Zunger A. Intrinsic n-type versus p-type doping asymmetry and the defect physics of ZnO. Phys Rev B, 2001, 63: 075205

[8] Yamamoto T, Yoshida H K. Solution using a codoping method to unipolarity for the fabrication of p-type ZnO. Jpn J Appl Phys, 1999, 38: 166

[9] Li J B, Wei S H. Design of shallow acceptors in ZnO: first-principles band-structure calculations. Phys Rev B, 2006, 74: 081201

[10] Yan Y, Zhang S B, Pantelides S T. Control of doping by impurity chemical potentials: predictions for p-type ZnO. Phys Rev Lett, 2001, 86: 5723
[11] Zhang S B, Wei S H. Nitrogen solubility and induced defect complexes in epitaxial GaAs:N. Phys Rev Lett, 2001, 86: 1789
[12] Yamamoto T. Codoping for the fabrication of p-type ZnO. Thin Solid Films, 2002, 420/421: 100
[13] Joseph M, Tabata H, Saeki H, et al. Fabrication of the low-resistive p-type ZnO by codoping method. Physica B, 2001: 302
[14] Vlasenflin T H, Tanaka M. P-type conduction in ZnO dual-acceptor-doped with nitrogen and phosphorus. Solid State Commun, 2007, 142: 292
[15] Krtschil A, Dadgar A, Oleynik N, et al. Local p-type conductivity in zinc oxide dual-doped with nitrogen and arsenic. Appl Phys Lett, 2005, 87: 262105
[16] Gai Y Q, Li J B, Li S S, et al. Design of shallow acceptors in ZnO through compensated donor-acceptor complexes: a density functional calculation. Phys Rev B, 2009, 80**:** 153201
[17] Liu B, Gu M, Liu X L, et al. First-principles study of fluorine-doped zinc oxide. Appl Phys Lett, 2010, 97: 122101
[18] Gai Y Q, Yao B, Wei Z P, et al. Effect on nitrogen acceptor as Mg is alloyed into ZnO. Appl Phys Lett, 2008, 92: 062110
[19] Kisi E, Elcombe M U. Parameters for the wurtzite structure of ZnS and ZnO using powder neutron diffraction. Acta Crystallographica Section C-Crystal Structure Communications, 1989, 45: 1867
[20] Perdew J P, Burke K, Ernzerhof M. Generalized gradient approximation made simple. Phys Rev Lett, 1996, 77: 3865
[21] Segall M D, Lindan P J D, Probert M J, et al. First-principles simulation: ideas, illustrations and the CASTEP code. Phys: Condens Matter, 2002, 14: 2717
[22] Wang X F, Chen X S, Dong R B, et al. Ferromagnetism in carbon-doped ZnO films from first-principle study. Phys Lett A, 2009, 373: 3091
[23] Shi L B, Chi F, Xu C Y. A first principles study on $m\mathrm{Al}_{\mathrm{Zn}}$–$n\mathrm{N}_{\mathrm{O}}$ complex doped ZnO. Chin Phys Lett, 2010, 27: 017102
[24] Nagare B J, Chacko S, Kanhere D G. Ferromagnetism in carbon-doped zinc oxide systems. J Phys Chem A, 2010, 114: 2689
[25] Sun J, Wang H T, He J L, et al. *Ab initio* investigations of optical properties of the high-pressure phases of ZnO. Phys Rev B, 2005, 71: 125132
[26] Chen X B, Qi L, Ma M Z, et al. Theoretical investigations of the electronic and optical properties of wurtzite and metastable rock-salt ZnO. Solid State Commun, 2008,145: 267
[27] Payne M C, Teter M P, Allan D C, et al. Iterative minimization techniques for ab initio total-energy calculations: molecular dynamics and conjugate gradients. Rev Mod Phys, 1992, 64: 1045
[28] Vanderbilt D. Soft self-consistent pseudopotentials in a generalized eigenvalue formalism. Phys Rev B, 1990, 417: 892
[29] Chowdhury R, Rees P, Adhikari S, et al. Electronic structures of silicon doped ZnO. Physica B, 2010, 405: 1981
[30] Janotti A, Segev D, Van de Walle C G. Effects of cation d states on the structural and electronic properties of III-nitride and II-oxide wide-band-gap semiconductors. Phys Rev B, 2006, 74: 045202
[31] Si P P, Su X Y, Hou Q Y, et al. First-principles calculation of the electronic band of ZnO doped with C. Journal of Semiconductors, 2009, 30: 052001
[32] Ranke W. Separation of the partial s- and p-densities of valence states of ZnO from UPS-measurements. Solid State Commun, 1976, 19: 685
[33] Schleife A, Fuchs F, Furthmuller J, et al. First-principles study of ground- and excited-state properties of MgO, ZnO, and CdO polymorphs. Phys Rev B, 2006, 73: 245212
[34] Vogel D, Kruger P, Pollmann J. *Ab initio* electronic-structure calculations for II–VI semiconductors using self-interaction-corrected pseudopotentials. Phys Rev B, 1995, 52: 14316
[35] Xu Y N, Ching W Y. Electronic, optical, and structural properties of some wurtzite crystals. Phys Rev B, 1993, 48: 4335
[36] Zuo C Y, Wen J, Zhu S L, et al. The effect of C–Al (Ga) codoping on p-type tendency in zinc oxide by first-principles. Opti Mater, 2010, 32: 595
[37] Anisimov V I, Aryasetiawan F, Lichtenstein A I. First-principles calculations of the electronic structure and spectra of strongly correlated systems: the LDA+U method. J Phys: Condens Matter, 1997, 9: 767
[38] Shirley R, Kraft M, Inderwildi O R. Electronic and optical properties of aluminium-doped anatase and rutile TiO_2 from *ab initio* calculations. Phys Rev B, 2010, 81: 075111
[39] Chen K, Fan G H, Zhang Y. First principles study of optical properties of wurtzite ZnO with Mn-doping. Acta Physica Sinica, 2008, 57: 1056 (in Chinese)
[40] Jaffe J E, Snyder J A, Lin Z, et al. LDA and GGA calculations for high-pressure phase transitions in ZnO and MgO. Phys Rev B, 2000, 62: 1660
[41] Freeout J L. Far-ultraviolet reflectance of II–VI compounds and correlation with the Penn—Phillips gap. Phys Rev B, 1973, 7: 3810
[42] Wen J, Zuo C Y, Xu M, et al. First-principles investigation of electronic structure and optical properties in N–F codoped ZnO with wurtzite structure. Eur Phys J B, 2011, 80: 30